Liquid Crystals
Publication details, including instructions for authors and subscription information:
http://www.informaworld.com/smpp/title~content=t713926090

Theory for the band structures in liquid crystal polymers under shear

B. J. A. Zielinska[a][b]; A. Ten Bosch[c]
[a] Institüt für Festkörperforschung, Jülich, F. R. Germany [b] Service de Physique du Solide et de Résonance Magnétique, Gif-sur-Yvette Cedex, France [c] Laboratoire de Physique de la Matière Condensée, Nice Cedex, France

To cite this Article Zielinska, B. J. A. and Bosch, A. Ten(1989) 'Theory for the band structures in liquid crystal polymers under shear', Liquid Crystals, 6: 5, 553 — 563
To link to this Article: DOI: 10.1080/02678298908034175
URL: http://dx.doi.org/10.1080/02678298908034175

LIQUID CRYSTALS, 1989, VOL. 6, NO. 5, 553–563

Theory for the band structures in liquid crystal polymers under shear

by B. J. A. ZIELINSKA†
Institüt für Festkörperforschung, KFA, D-5170 Jülich, F.R. Germany

and

A. TEN BOSCH
Laboratoire de Physique de la Matière Condensée, CNRS L.A. 190, Parc Valrose,
06034 Nice Cedex, France

(*Received 11 December 1988; accepted 13 June 1989*)

A theory for the shear flow instability in a liquid crystal aligned by the initial flow is presented. We have investigated a periodic distortion of the director and the velocity field in the plane perpendicular to the velocity gradient. We present solutions for the director and velocity field and make a connection with the optical image observed under a polarizing microscope. We include the convective terms in the basic equations neglected previously, and show that they alter the values of the critical parameters, but do not change the instability mechanism. Comparison with experimental data is made and further experiments are suggested.

1. Introduction

It is well-known that sheared liquid crystal polymer systems demonstrate typical striped textures under the polarizing microscope [1–8]. These textures are primarily observed as a relaxation phenomenon in the liquid film shortly after the shear stress has been removed. Often the structure persists into the dried solid as in commercially spun fibres of liquid crystal polymers [6]. A clear explanation of this phenomenon has not yet been given. Careful optical experiments have shown that the textures occur due to a depth dependent distortion of the average direction of orientation of the macromolecules perpendicular to the shear plane [2]. The importance of various parameters has been indicated: the molecular weight [3], the sample thickness [5], the shear rate [1], the time during which the shear stress was applied [8] and the total shear deformation [5]. A connection with the rheological properties has also been demonstrated and in particular to the first normal stress difference which seems to change sign when the band structures appear [1].

Various theoretical models have been proposed. Orientation of the directors within alternate planes by creation of alignment-inversion walls has been invoked [1]. Subsequent experiments seem to indicate rather a smooth transition of the orientation between domains of a given direction [2]. The tumbling instability has been suggested as an explanation [4] but would not fulfill this condition. In liquid crystal polymers, novel instabilities of the director pattern have recently been observed in electric and magnetic fields. These were shown to occur under certain conditions for the Frank

---

† Present address: Service de Physique du Solide et de Résonance Magnétique, C.E.N. Saclay, 91191 Gif-sur-Yvette Cedex, France.

0267–8292/89 $3.00

elastic constants expected in polymeric systems [9]. It has been proposed that a similar mechanism could explain the band textures in a shear flow field.

As yet, due to the difficulty of observing the band pattern during flow, it is not certain, experimentally, whether the band textures occur because of the onset of an instability at a certain critical shear threshold. Some authors consider a rather pure relaxation process via a periodic director distortion after the shear flow [7] has ceased. According to this picture the macromolecules are stretched in the field and then relax back to a coiled state. It is not clear however which mechanism in the relaxation process is responsible for the observed periodic structure. On the other hand recent experiments indicate that the shear threshold is inversely proportional to the sample thickness [5]. This agrees with the scaling argument presented in the following sections (see relations (3.1)) and thus supports the instability idea.

Hydrodynamic instabilities in conventional liquid crystals have been well studied and good agreement between experiment and theory has been obtained. The theory is based on the Leslie–Ericksen formulation of orientation dependent viscoelasticity and primary distortion of the director within the shear plane was considered [10]. In the following sections we shall use the same formalism to describe polymer liquid crystals as well. We have investigated [11] the existence of an instability producing a periodic pattern with a distortion perpendicular to the shear plane as observed in the optical experiments. We use the Leslie–Ericksen theory which is successful in describing electrohydrodynamic instabilities in polymer liquid crystals [12] and should contain the essential physical phenomena. We work within the framework of linear stability analysis and obtain the critical shear rate and the critical wavevector for the instability to occur. We present here the total velocity and director fields. We also make a connection with the optical properties, such as the scattered light intensity observed by a polarizing microscope.

2. The model

We consider a layer of nematic fluid enclosed between two parallel plates. One of the plates moves relative to the other with a constant velocity inducing a constant shear rate, s. Such a system is described by the usual equations for the nematic liquid crystal [10] consisting of the torque and force conservation equations. The momentum conservation is

$$\boldsymbol{\Gamma}^{\text{tot}} = \boldsymbol{\Gamma}^{\text{e}} + \boldsymbol{\Gamma}^{\text{v}} = 0. \qquad (2.1)$$

Here $\boldsymbol{\Gamma}^{\text{e}}$ is the elastic torque defined by

$$\boldsymbol{\Gamma}^{\text{e}} = \mathbf{n} \times (\mathbf{h}_S + \mathbf{h}_T + \mathbf{h}_B) \qquad (2.2)$$

and

$$\begin{aligned} \mathbf{h}_S &= K_1 \nabla(\nabla \cdot \mathbf{n}), \\ \mathbf{h}_T &= -K_2\{A \nabla \times \mathbf{n} + \nabla \times (A\mathbf{n})\}, \\ \mathbf{h}_B &= K_3\{\mathbf{B} \times \nabla \times \mathbf{n} + \nabla \times (\mathbf{n} \times \mathbf{B})\}, \\ A &= \mathbf{n} \cdot (\nabla \times \mathbf{n}), \qquad \mathbf{B} = \mathbf{n} \times (\nabla \times \mathbf{n}) \end{aligned}$$

are components of the molecular field for the splay, twist and bend distortion, respectively. Here $\mathbf{n}$ denotes the director field, and K_1, K_2 and K_3 are elastic constants. $\boldsymbol{\Gamma}^{\text{v}}$ is the viscous torque defined by

$$\boldsymbol{\Gamma}^{\text{v}} = -\mathbf{n} \times \mathbf{h}_{\text{v}}, \qquad (2.3)$$

where $\mathbf{h}_v$ is the viscous molecular field

and

$$\mathbf{h}_v = \gamma_1 \mathbf{N} + \gamma_2 \mathbf{A} \cdot \mathbf{n},$$

$$\mathbf{N} = \frac{d\mathbf{n}}{dt} - \tfrac{1}{2}(\nabla \times \mathbf{v}) \times \mathbf{n}, \qquad \frac{d}{dt} = \partial_t + \mathbf{v} \cdot \nabla,$$

$$A_{ij} = \tfrac{1}{2}(\partial_i v_j + \partial_j v_i).$$

Here $\mathbf{v}$ is the velocity field, $\gamma_1 = \alpha_3 - \alpha_2$, $\gamma_2 = \alpha_3 + \alpha_2$, α_2 and α_3 are the rotational viscosities. The force conservation equation has the form

$$\varrho \frac{d}{dt} v_i = -\partial_i p + \partial_j(\sigma'_{ij} + \sigma^e_{ij}), \tag{2.4}$$

where σ'_{ij} is the viscous part of the Leslie–Ericksen stress tensor

$$\sigma'_{ij} = \alpha_1 n_i n_j (n_k A_{kl} n_l) + \alpha_2 n_i N_j + \alpha_3 n_j N_i + \alpha_4 A_{ij} + \alpha_5 n_i n_k A_{kj} + \alpha_6 A_{ik} n_k n_j;$$

$\alpha_1 \ldots \alpha_6$ are the Leslie coefficients, p in the hydrostatic pressure and ϱ in the density. σ^e_{ij} is the elastic stress tensor, which is at least second order in $\partial_i n_k$. Since in what follows we shall be concerned only with linear stability, σ^e_{ij} will be omitted.

In the following we assume that $\alpha_3/\alpha_2 > 0$. In this case these equations have a steady state solution: $tg\phi = \sqrt{(\alpha_3/\alpha_2)}$ independent of the shear rate, where ϕ is the angle in the plane of the velocity gradient formed by the director and the shear direction. In the present work we are concerned with a layer of fluid unbound horizontally, but of finite thickness in the perpendicular direction. We neglect boundary effects [14] and assume that the liquid crystal molecules are basically free to form an angle with the bounding plates. The layer of fluid is taken to extend in the xy plane. We denote small perturbations from the steady state solution by

$$(n'_x, n'_y, n'_x) = (0, \cos\phi, \sin\phi) + (n_x, n_y, n_z)$$

$$v = (0, sz, 0) + (v_x, v_y, v_z).$$

In order to perform the linear stability analysis we linearize equations (2.1) and (2.4) in perturbations around the steady state. As the result of linearization we obtain two decoupled sets of equations: one for n_x and v_x and the other for the y and z components of the velocity and director fields. The equations for the x components have been derived previously [11] and are

$$[-(\alpha_3 - \alpha_2)(\partial_t + sz\partial_y) + K_2 D_-^2 + K_3 D_+^2 + \alpha_2 s tg\phi] n_x - \alpha_2 D_+ v_x = 0, \tag{2.5 a}$$

$$[\alpha_2 D_+ / s(\partial_t + sz\partial_y) + \alpha_1 \cos\phi \sin\phi D_+ + \tfrac{1}{2}\alpha_6(\sin\phi\partial_y + \cos\phi\partial_z) + \tfrac{1}{2}\alpha_3 D_-] s n_x$$
$$+ [-\varrho(\partial_t + sz\partial_y) + \tfrac{1}{2}(\alpha_5 - \alpha_2) D_+^2 + \tfrac{1}{2}\alpha_4(\partial_y^2 + \partial_z^2)] v_z = 0, \tag{2.5 b}$$

where

and

$$D_+ = \cos\phi\partial_y + \sin\phi\partial_z$$

$$D_- = \cos\phi\partial_z - \sin\phi\partial_y$$

Here we have used the fact that the y and z components of the total torque are not independent to first order: $\Gamma_y^{\text{tot}}/\sin\phi = -\Gamma_z^{\text{tot}}/\cos\phi$. In equations (2.5 *a*) and (2.5 *b*) and in what follows we drop the derivatives with respect to x, since we are only interested in solutions uniform in the x direction.

Using the fact that $\mathbf{n}^2 = 1$ we conclude that to first order in the perturbations n_y and n_z are not independent: $\cos\phi n_y = \sin\phi n_z$ and find for the x component of the total torque

$$\begin{aligned}\Gamma_x^{\text{tot}} = & -\{2\cos\phi\sin\phi[s\gamma_2 + (K_1 - K_3)\partial_{zy}] + [\cos^2\phi K_3 + \sin^2\phi K_1]\partial_y^2 \\ & + [\sin^2\phi K_3 + \cos^2\phi K_1]\partial_z^2\}n_y/\sin\phi + \gamma_1\partial_y v_z \\ & + \gamma_2\cos\phi\sin\phi(\partial_y v_y - \partial_z v_z) = 0.\end{aligned} \tag{2.6}$$

The y and z components of the force equations have the form

$$\varrho(\partial_t + sz\partial_y)v_y = -\partial_y p + \partial_y\sigma'_{yy} + \partial_z\sigma'_{zy}, \tag{2.7 a}$$

$$\varrho(\partial_t + sz\partial_y)v_z = -\partial_z p + \partial_y\sigma'_{yz} + \partial_z\sigma'_{zz}, \tag{2.7 b}$$

where σ'_{ij} $(i, j = y, z)$ depend on n_y, n_z, v_y and v_z. The corresponding expressions for the components of the stress tensor are rather lengthy and are given in Appendix A.

3. Solution and results

As before [11] we introduce the dimensionless variables

$$\bar{v}_x = \frac{|\alpha_2|}{K_2}av_x, \quad \bar{t} = \frac{K_2}{|\alpha_2|a^2}t, \quad \bar{s} = \frac{a^2|\alpha_2|}{K_2}s, \quad \bar{z} = \frac{z}{a} \quad \text{and} \quad \bar{y} = \frac{y}{a}, \tag{3.1}$$

where a is the sample thickness. If the convective terms, which depend explicitly on z are neglected in equations (2.5 a–b), the solutions of equations (2.5 a–b) periodic in the shear direction are of the form

$$\begin{pmatrix} n_x \\ \bar{v}_x \end{pmatrix} = \sum_k \exp(\bar{\sigma}\bar{t} + ik\bar{y}) \sum_{j=1}^{4} \begin{pmatrix} n_j^o \\ v_j^o \end{pmatrix} A_j \exp(iq_j\bar{z}) + \text{c.c.}, \tag{3.2}$$

where q_j are the roots of the characteristic polynomial. The solution in the presence of the convective terms and the influence of the terms explicit in z on the values of the critical parameters are discussed in Appendix B. Inserting equation (3.2) into equations (2.5 a–b) and using the boundary conditions

$$\bar{v}_x = n_x = 0 \quad \text{at} \quad \bar{z} = \pm\tfrac{1}{2}, \tag{3.3}$$

we obtain the shear rate $\bar{s}$ as a function of the wavevector k and the frequency $\bar{\sigma}$. We found [11], that for a wide range of parameters of interest the instability is stationary, i.e. $\bar{\sigma} = 0$. Finally $\bar{s}$ was minimized with respect to k, giving the critical values s_{cr} and k_{cr} for two cases: the liquid crystal 4-methoxybenzilidene-4′-n-butylaniline (MBBA) [13] and the polymer liquid crystal in solution polybenzyl glutamate (PBG) [15]. We found for a sample of thickness of 100 μm $s_{\text{cr}} = 19{\cdot}5\ \text{s}^{-1}$ and $k_{\text{cr}} = 3{\cdot}1$ for MBBA and $s_{\text{cr}} = 0{\cdot}064\ \text{s}^{-1}$ and $k_{\text{cr}} = 0{\cdot}85$ for PBG in solution. This is in agreement with experiments which show that a high degree of polymerization favours the formation of band textures [3].

Using the values of the critical parameters calculated from equations (2.5 a–b) for n_x and v_x we now construct the solutions for n_y, n_z, v_y and v_z. Equations (2.6) and (2.7 a–b) together with the incompressibility condition

$$\partial_y v_y + \partial_z v_z = 0 \tag{3.4}$$

form a set of four equations for the unknown functions n_y, v_y, v_z and p (n_z and n_y are not independent to first order and $n_z\sin\phi = n_y\cos\phi$). Since we are only interested in solutions periodic in the y direction we can write, similarly to equation (3.2),

$$\begin{pmatrix} n_y \\ v_y \\ v_z \\ p \end{pmatrix} = \sum_k \exp(ik\bar{y}) \sum_{j=1}^{6} \begin{pmatrix} n^o_{yj} \\ v^o_{yj} \\ v^o_{zj} \\ p^o_j \end{pmatrix} \cdot B_j \exp(ir_j\bar{z}) + \text{c.c.}, \qquad (3.5)$$

where r_j are the roots of the sixth order characteristic polynomial obtained by substituting equations (2.6), (2.7 *a*) and (3.4) into (2.7 *b*). Here we have already taken into account that $\bar{\sigma} = 0$. For a given choice of K_i and α_i solution (3.5) depends on s_{cr} and k_{cr}. The amplitudes B_j can be calculated by inserting equation (3.5) into the boundary conditions for n_y, v_y and v_z. Assuming stick boundary conditions for the velocity field we impose

$$v_y(-\tfrac{1}{2}) = v_y(\tfrac{1}{2}) = v_z(-\tfrac{1}{2}) = v_z(\tfrac{1}{2}) = 0. \qquad (3.6)$$

We assume that the director can adjust at the plates and therefore impose free boundary conditions for the director in the shear plane

$$n_y/n_z = -(\mathrm{tg}\,\phi)^{-1} \quad \text{for} \quad \bar{z} = \pm\tfrac{1}{2}. \qquad (3.7)$$

We have calculated the director and velocity fields n_y, n_z, v_y and v_z for the critical shear rate and critical wavevector, the elastic constants K_i and the Leslie coefficients α_i corresponding to the case of a lyotropic polymer liquid crystal in solution namely PBG. The resulting director profile in the xy plane (for $\bar{z} = -0\cdot25$) is shown in figure 1. In this figure we can see a periodic change of the director in the y direction, as assumed in equations (3.2) and (3.5). Such a director pattern is consistent with the optical image obtained from the band structure, as will be discussed later. The corresponding velocity profile has a similar form and is also periodic in y, but shifted in phase with respect to the director field. In figure 2 the velocity field in the shear plane (yz plane) due to the perturbations around the steady state constant shear

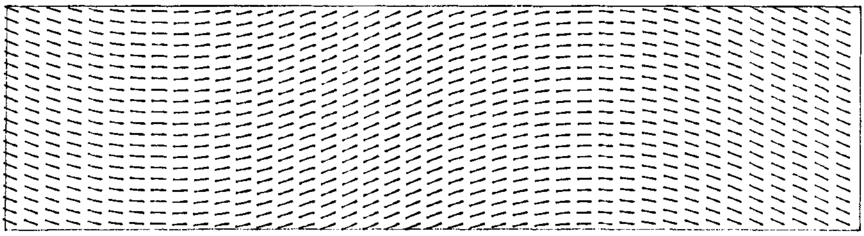

Figure 1. Director field in the xy plane (perpendicular to the shear plane) for $\bar{z} = -0\cdot25$.

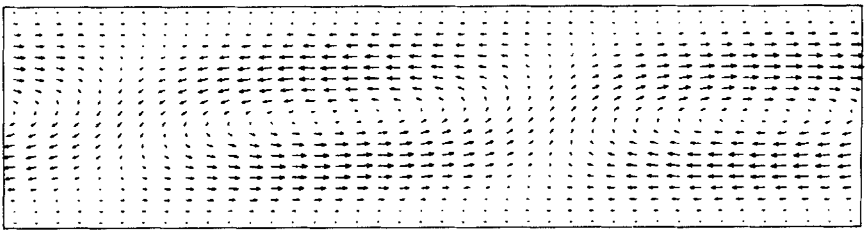

Figure 2. Perturbations in the velocity field around the steady state constant shear profile in the yz plane (the shear plane).

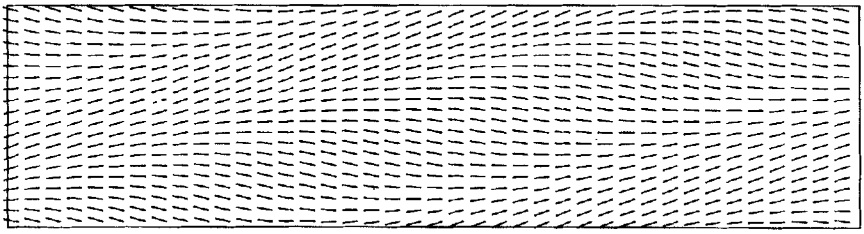

Figure 3. Director field in the yz plane (the shear plane).

profile is shown. It can be concluded from this figure, that the band structure instability will impose a roll pattern on the primary constant shear velocity field. Finally in figure 3 the director pattern in the shear plane is presented. The deviations from the steady state shown in all of the figures are in arbitrary units. The linear theory presented here permits us to calculate the solutions up to a constant. Consequently in figures 1, 2 and 3 we have chosen the units such that the deviations from the steady state pattern are clearly visible.

If the director cannot adjust at the plates, the boundary conditions (3.7) become $n_y = n_z = 0$ at $\bar{z} = \pm 1/2$ and only the trivial solution (i.e. $v_y = v_z = n_y = n_z = 0$) is possible. In this case the velocity and director profile in the yz plane are not perturbed. Careful consideration of surface effects is necessary to choose the solution which corresponds to a given director pattern. Experimentally this would be defined by spontaneous anchoring at the surface or pretreatment of the glass plates.

4. Optical properties

The image observed in a polarizing microscope can be expressed [16] as

$$I(\mathbf{r}) \sim |(\alpha(\mathbf{r}) \cdot \mathbf{P}) \cdot \mathbf{A}|^2, \tag{4.1}$$

where **P** is the unit vector of the direction of the polarizer, **A** that of the direction of the analyser and $\alpha(\mathbf{r})$ is the polarization tensor of the sample. Let xy be the plane of observation for crossed polarizers $\mathbf{A} = (1, 0)$, $\mathbf{P} = (0, 1)$. The polarization tensor of the sample is

$$\alpha_{ij} = \alpha\delta_{ij} + \alpha_a n_i^t n_j^t, \tag{4.2}$$

where α is the average and α_a the anisotropy of polarization. The scattered light intensity at position (y, z) is then

$$I(y, z) \sim (\alpha_a n_x^t n_y^t)^2. \tag{4.3}$$

Flow alignment is generated under shear but in real samples the degree of orientation is not perfect, and the sample appears birefringent. Perfect alignment gives the total scattered light intensity of the sample relative to the perturbation n_x as

$$I(y) \sim \alpha_a \cos^2 \phi \int dz |n_x(y, z)|^2. \tag{4.4}$$

We have evaluated this integral using the expression for n_x obtained in §3 and the result is shown in figure 4. A smooth periodic function is obtained, in agreement with optical measurements. The image is given by a series of parallel dark and light lines

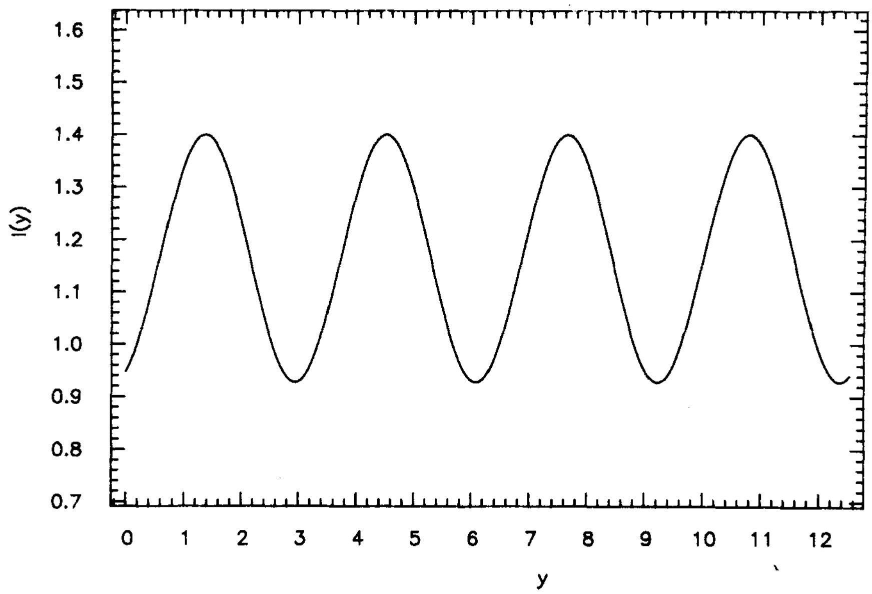

Figure 4. Scattered light intensity according to equation (4.6) (in arbitrary units).

perpendicular to the shear direction. Note that the director fluctuation following from our theory is of the form

$$n_x = a(z)\cos ky + b(z)\sin ky = \sin(ky + \psi(z)). \qquad (4.5)$$

A large depth dependent phase shift $\psi(z)$ could blur or even destroy the periodicity of the image in the polarizing microscope during shear. If $n_x(z)$ relaxes rapidly on stopping the shear, the pattern would appear then as a relaxation phenomenon.

In microscopy experiments the sample can be rotated by an angle Ω relative to the analyser and the change in the transmitted light intensity can be observed. The formula for the scattered light intensity in this case is

$$I(y) \sim \alpha_a \sin^4 \phi \int dz \sin^2(2\beta(y, z)), \qquad (4.6)$$

where $\mathrm{tg}\,\beta \sim n_x/\sin\phi$ if the analyser is aligned in the shear direction and $\beta \to \beta + \Omega$ on rotation. The periodic variation in the orientation of the optic axis can then be used to explain the motion of the extinction bands on rotation of the crossed polars, the variation of the total intensity $\int dyI(y)$ and the analysis of the conoscopic [2] image.

5. Discussion

We have presented here a theory for band structures in liquid crystal polymers under shear. These band structures are a common phenomenon in liquid crystal polymers and occur in different geometries and for different types of molecules. It is plausible therefore to assume that the origin of this phenomenon is not material specific. In the present work we argue [11] that for simple shear flow the band structures are due to an instability mechanism present in the Leslie–Ericksen equations. Band structures have also been observed in other types of flows, as for example elongational flow. It remains to be shown if an instability similar to the one presented here could be found for other types of flow. We have calculated the critical shear rate and wavevector for this instability and present the director and velocity fields. The Leslie–Ericksen formulation does not taken into account the viscoelastic nature of the macromolecules. However, as for other hydrodynamic instabilities [18, 19] we can argue, that the viscoelastic properties will very likely alter the values of the critical parameters, but will not destroy the instability mechanism. In the previous calculation [11] the inertial terms in the equation were neglected. In the present work we have included these terms and have shown that they introduce a quantitative change to the critical parameters, but qualitatively the instability remains the same. Our calculations show that the values of the critical shear and wavevector depend strongly on the choice of the elastic constants and the anisotropic viscosities. As for most polymer liquid crystals these parameters are not very well-known and the values for s_{cr} and k_{cr} predicted here have only a qualitative character. In particular we hope that more accurate values of these parameters and taking into account the viscoelastic properties of the polymers would result in larger values of the critical wavevector, in better agreement with the experimental data.

Many of the liquid crystal polymer systems are cholesteric and not nematic as assumed here. The cholesteric structure is expected to unwind as the molecules align on application of shear, leading to a nematic phase. However, cholesterics usually have a lower elastic constant for twist (K_2), than nematics. In our theory lower K_2 favours the formation of the band structure by lowering the value of the critical shear, as can be seen from the scaling relations (3.1). The out of shear plane distortion of the director (i.e. non-zero n_x) is a twist and is essential for the instability to occur. Therefore cholesterics are expected to form the bands at lower shear than nematics. Secondary structures have been observed in cholesterics upon relaxation of the band pattern [20]. These structures may be due to the inherent periodicity in these materials (the pitch of the helix). The rheology of cholesteric polymers is still being developed but a straight forward extension of the present model could be envisaged.

The solutions for the director and velocity fields in the shear plane presented here depend on the boundary conditions for the director at the plates. To our knowledge the experiments on polymer liquid crystals in which the band structures have been observed did not use pretreated plates. We have therefore imposed free boundary conditions on the director in the shear plane. Mechanical pretreating plates or orientation in a magnetic field could also be used in samples of polymer liquid crystals and its influence on band forming could be determined experimentally. In addition the dependence of the critical shear rate [5] and the critical wavevector on the thickness of the sample should be elucidated further. In particular, the scaling relation (3.1) predicts that the critical shear rate decreases as the square of the sample thickness.

Different boundary conditions for the director in the out of shear plane could be proposed. Here we have used stick boundary conditions for n_x, amounting to n_x being zero at the plates while the derivative $\partial_z n_x$ is left free to adjust. Alternatively for the case of unpretreated surfaces we could study torque free boundary conditions in which the derivative $\partial_z n_x$ is put to zero at the plates and the director is left free to adjust.

Finally it would be interesting to study the band structures in polymer liquid crystals theoretically and experimentally in geometries different from the simple shear geometry. The Taylor column is a suitable candidate, because of the existing theoretical framework and a possibility of continuous shear, which should allow the observation of the bands under shear conditions.

Appendix A

The components of the Leslie–Ericksen stress tensor can be calculated from the definition of σ'_{ij} following equation (4)

$$\begin{aligned}\sigma'_{yy} = {} & \{\alpha_1 \cos^3\phi \sin\phi + \gamma_2 \cos\phi z\partial_y + \tfrac{1}{2}(\alpha_5 + \alpha_6)\sin\phi - \tfrac{1}{2}\gamma_2 \sin\phi\} s n_y \\ & + \{\alpha_1 \cos^2\phi - \tfrac{1}{2}\gamma_2 + \tfrac{1}{2}(\alpha_5 + \alpha_6)\}\cos\phi s n_z \\ & + \{\alpha_1 \cos^3\phi D_+ - \tfrac{1}{2}\gamma_2 \sin\phi\cos\phi\partial_z + \tfrac{1}{2}\alpha_4\partial_y \\ & + (\alpha_5 + \alpha_6)(\sin\phi\partial_z + \cos\phi\partial_y)\cos\phi\} v_y \\ & + \{\alpha_1 \cos\phi D_+ + \tfrac{1}{2}\gamma_2\partial_y + \tfrac{1}{2}(\alpha_5 + \alpha_6)\partial_y\}\sin\phi\cos\phi v_z,\end{aligned} \tag{A 1}$$

$$\begin{aligned}\sigma'_{zz} = {} & \{\alpha_1 \sin^3\phi \cos\phi + \gamma_2 \sin\phi z\partial_y + \tfrac{1}{2}(\alpha_5 + \alpha_6)\cos\phi + \tfrac{1}{2}\gamma_2 \cos\phi\} s n_z \\ & + \{\alpha_1 \sin^2\phi + \tfrac{1}{2}\gamma_2 + \tfrac{1}{2}(\alpha_5 + \alpha_6)\}\sin\phi s n_y \\ & + \{\alpha_1 \sin^3\phi D_+ - \tfrac{1}{2}\gamma_2 \sin\phi\cos\phi\partial_y + \tfrac{1}{2}\alpha_4\partial_z \\ & + (\alpha_5 + \alpha_6)(\sin\phi\partial_z + \cos\phi\partial_y)\sin\phi\} v_z \\ & + \{\alpha_1 \sin\phi D_+ + \tfrac{1}{2}\gamma_2\partial_z + \tfrac{1}{2}(\alpha_5 + \alpha_6)\partial_z\}\sin\phi\cos\phi v_y,\end{aligned} \tag{A 2}$$

$$\begin{aligned}\sigma'_{zy} = {} & \{2\alpha_1 \sin^2\phi \cos\phi + \alpha_2 \sin\phi z\partial_y + \alpha_3 \cos\phi + \alpha_6 \cos\phi\} s n_y \\ & + \{2\alpha_1 \cos^2\phi \sin\phi + \alpha_3 \cos\phi z\partial_y - \alpha_2 \sin\phi + \alpha_5 \sin\phi\} s n_z \\ & + \{\alpha_1 \cos^2\phi \sin\phi D_+ + \tfrac{1}{2}(\alpha_2 \sin^2\phi + \alpha_3 \cos^2\phi)\partial_z \\ & + \tfrac{1}{2}\alpha_4\partial_z + \alpha_5 \cos\phi\sin\phi\partial_y + \tfrac{1}{2}(\alpha_5 \sin^2\phi + \alpha_6 \cos^2\phi)\partial_z\} v_y \\ & + \{\alpha_1 \sin^2\phi \cos\phi D_+ + \tfrac{1}{2}(\alpha_2 \sin^2\phi - \alpha_3 \cos^2\phi)\partial_y \\ & + \tfrac{1}{2}\alpha_4\partial_y + \alpha_6 \cos\phi\sin\phi\partial_z + \tfrac{1}{2}(\alpha_5 \sin^2\phi + \alpha_6 \cos^2\phi)\partial_y\} v_z,\end{aligned} \tag{A 3}$$

$$\begin{aligned}\sigma'_{yz} = {} & \{2\alpha_1 \sin^2\phi \cos\phi + \alpha_3 \sin\phi z\partial_y + \alpha_2 \cos\phi + \alpha_5 \cos\phi\} s n_y \\ & + \{2\alpha_1 \cos^2\phi \sin\phi + \alpha_2 \cos\phi z\partial_y - \alpha_3 \sin\phi + \alpha_6 \sin\phi\} s n_z \\ & + \{\alpha_1 \cos^2\phi \sin\phi D_+ + \tfrac{1}{2}(-\alpha_3 \sin^2\phi + \alpha_2 \cos^2\phi)\partial_z \\ & + \tfrac{1}{2}\alpha_4\partial_z + \alpha_6 \cos\phi\sin\phi\partial_y + \tfrac{1}{2}(\alpha_6 \sin^2\phi + \alpha_5 \cos^2\phi)\partial_z\} v_y \\ & + \{\alpha_1 \sin^2\phi \cos\phi D_+ + \tfrac{1}{2}(\alpha_3 \sin^2\phi - \alpha_2 \cos^2\phi)\partial_y \\ & + \tfrac{1}{2}\alpha_4\partial_y + \alpha_5 \cos\phi\sin\phi\partial_z + \tfrac{1}{2}(\alpha_6 \sin^2\phi + \alpha_5 \cos^2\phi)\partial_y\} v_z.\end{aligned} \tag{A 4}$$

Appendix B

If the terms explicit in z cannot be neglected in equations (5*a–b*), then the solution of these equations can no longer be written as sum of exponentials shown in equation (9). In this case the dependence in the z direction is more complicated and a solution periodic in the y direction will have the form

$$\begin{pmatrix} n_x \\ \bar{v}_x \end{pmatrix} = \sum_k \exp(\bar{\sigma}\bar{t} + ik\bar{y}) \begin{pmatrix} f(z) \\ g(z) \end{pmatrix} + \text{c.c.}, \tag{B 1}$$

where the functions $f(z)$ and $g(z)$ have to be determined by numerical integration. We briefly sketch the numerical integration method. Equations 5(*a–b*) can be written in the form of our first order differential equations with respect to z

$$\frac{d}{d\bar{z}}\begin{bmatrix} n_x \\ m_x \\ \bar{v}_x \\ \bar{w}_x \end{bmatrix} = \mathscr{M}(\bar{z}, \bar{s}, k, \bar{\sigma}; K_i, \alpha_i)\begin{bmatrix} n_x \\ m_x \\ \bar{v}_z \\ \bar{w}_x \end{bmatrix}, \tag{B 2}$$

where $m_x = (d/d\bar{z})n_x$, $\bar{w}_x = (d/d\bar{z})\bar{v}_x$, K_i stands for K_2, K_3 and α_i for $\alpha_1, \ldots, \alpha_6$. The matrix $\mathscr{M}$ depends explicitly on $\bar{z}$, but does not contain derivatives with respect to $\bar{z}$. Using arbitrary boundary conditions for m_x and $\bar{w}_x$ at $\bar{z} = -\frac{1}{2}$ it is possible to construct a solution satisfying

$$n_x(-\tfrac{1}{2}) = \bar{v}_x(-\tfrac{1}{2}) = 0 \quad \text{and} \quad n_x(\tfrac{1}{2}) = 0.$$

The value of $\bar{v}_x$ at $\bar{z} = \frac{1}{2}$ defines a function F

$$F(\bar{s}, k, \bar{\sigma}; K_i, \alpha_i) = v_x(\tfrac{1}{2}). \tag{B 3}$$

The set of equations (B 2) can then be solved numerically using the Runge–Kutta method of order four and the values of $\bar{\sigma}$, k and $\bar{s}$ can be chosen such that

$$F(\bar{s}, k, \bar{\sigma}; K_i, \alpha_i) = 0 \tag{B 4}$$

using the Newton–Raphson method.

We have calculated the critical parameters $\bar{s}$, $\bar{\sigma}$ and k for several sets of values of K_i and α_i. We found that the convective terms change the values of the critical parameter $\bar{s}_{cr}$ and k_{cr}, but the transition stays stationary, i.e. $\bar{\sigma} = 0$ in all of the cases considered. However we have encountered numerical difficulties for some values of the parameters. These numerical difficulties appear while calculating $F = 0$ as defined in equation (B 4) and have been previously encountered in numerical calculations of initial value problems [17]. They can already be anticipated from inspection of equation (9). If one of the q_js has a large imaginary part, such that $iq_j\bar{z} > 0$ for $\bar{z} > 0$, then this q_j will dominate the solution. In the Newton–Raphson method $F = 0$ is found by combining two linearly independent solutions, which in practice means subtracting two large numbers. Consequently large $\mathrm{Re}\,(iq_j)$ requires high precision, which can exceed double or even quadrupole precision. When solution (9) is applicable we have found in most cases that for the largest q_j $\mathrm{Re}\,(q_j)$ is of the order of 20. In the situation when solution (B 1) is applicable, q_j cannot be evaluated, but in some cases we have found that the available precision was not sufficient. In order to determine the values of the critical parameters in these cases more sophisticated methods of integration should be applied [17].

With this method and for the set of realistic parameter values for PBG [15] ($K_2 = 0{\cdot}36 \times 10^{-7}$, $K_3 = 0{\cdot}4 \times 10^{-6}$, $\alpha_1 = -31$, $\alpha_2 = -33$, $\alpha_3 = -0{\cdot}16$, $\alpha_4 = 1{\cdot}2$, $\alpha_5 = 26$ and $\alpha_6 = -0{\cdot}9$) we found $\bar{s}_{cr} = 1{\cdot}092 \times 10^4$ and $k_{cr} = 1{\cdot}95$. This gives for a sample thickness of 100 μm a critical shear rate $s_{cr} = 0{\cdot}112\,\mathrm{s}^{-1}$ and periodicity of the pattern slightly larger than the thickness of the sample. This should be compared with $s_{cr} = 0{\cdot}064\,\mathrm{s}^{-1}$ reported in [11].

We conclude, that inclusion of the convective terms in the equations changes the values of the critical parameters, but it does not change the nature of the transition. For some values of the material parameters more sophisticated numerical methods should be employed in order to avoid numerical difficulties.

References

[1] Kiss, G., and Porter, R. S., 1980, *Molec. Crystals liq. Crystals*, **60**, 267.

[2] Viney, C., Donald, A. M., and Windle, A. H., 1983, *J. mat. Sci.*, **18**, 1136.

[3] Graziano, D. J., and Mackely, M. R., 1984, *Molec. Crystals liq. Crystals*, **108**, 73.

[4] Marrucci, G., 1985, *Pure appl. Chem.*, **57**, 1545.

[5] Marrucci, G., Grizzuti, N., and Buonaurio, A., 1987, *Molec. Crystals liq. Crystals*, **153**, 263.

[6] Viney, C., and Windle, A. H., 1987, *Phil. Mag.* A, **55**, 463.

[7] Ernst, B., and Navard, P., 1989, *Macromolecules* (to be published).

[8] Marsano, E., Carpaneto, L., and Cifferi, A., 1989, *Molec. Crystals liq. Crystals* (to be published).

[9] Hurd, A. J., Fraden, S., Lonberg, F., and Mayer, R. B., 1985, **46**, 905.

[10] Manneville, P., and Dubois-Violette, E., 1976, *J. Phys.*, **37**, 285.

[11] Zielinska, B. J. A., and ten Bosch, A., 1988, *Phys. Rev.* A, **38**, 5465.

[12] Gilli, J. M., Pinton, J. F., ten Bosch, A., and Sixou, P., 1986, *Molec. Crystals liq. Crystals*, **132**, 149.

[13] Stephen, M., and Straley, J., 1974, *Rev. mod. Phys.*, **46**, 617.

[14] Leslie, F., 1968, *Proc. R. Soc.* A, **307**, 359.

[15] Meyer, R. B., Lonberg, F., Taratuta, V., Fraden, S., Lee, Sin-Doo and Hurd, A. J., 1985, *Faraday Discuss. chem. Soc.*, **79**, 125.

[16] Tanaka, H., Hayashe, T., and Nishi, T., 1986, *J. appl. Phys.*, **59/11**, 3627.

[17] Drazin, P. G., and Reid, W. H., 1981, *Hydrodynamic Stability* (Cambridge University Press), pp. 208–211.

[18] Zielinska, B. J. A., 1988, *Convection in Viscoelastic Fluids, Proceedings of the Workshop of Propagation in Nonequilibrium Systems*, Les Houches, France, edited by J. E. Wesfried *et al.* (Springer).

[19] Zielinska, B. J. A., and Demay, Y., 1988, *Phys. Rev.* A, **38**, 897.

[20] Fried, F., and Sizou, P., 1988, *Molec. Crystals liq. Crystals*, **158**, 163.